Materials and Design 90 (2016) 852–857

Contents lists available at ScienceDirect

Materials and Design

journal homepage: www.elsevier.com/locate/matdes

Label-free electronic detection of interleukin-6 using horizontally aligned carbon nanotubes

Hu Chen [a,b,d], Teck Kian Choo [a], Jingfeng Huang [a,b], Yi Wang [c], Yuanjun Liu [c], Mark Platt [d], Alagappan Palaniappan [c], Bo Liedberg [a,c], Alfred Iing Yoong Tok [a,b,*]

[a] School of Materials Science and Engineering, Nanyang Technological University, 639798, Singapore
[b] Institute for Sports Research, Nanyang Technological University, 50 Nanyang Avenue, 639798, Singapore
[c] Centre for Biomimetic Sensor Science, 50 Nanyang Drive, 637553, Singapore
[d] Department of Chemistry, Centre for Analytical Science, Loughborough University, Loughborough, Leicestershire LE11 3TU, UK

ARTICLE INFO

Article history:
Received 3 March 2015
Received in revised form 5 November 2015
Accepted 7 November 2015
Available online 10 November 2015

Keywords:
Interleukin-6
Field-effect transistor
Horizontally aligned single-walled carbon nanotubes

ABSTRACT

A facile, sensitive, and label-free assay for detection of interleukin-6 (IL-6) using liquid-gated field-effect transistor (FET) sensors based on horizontally aligned single-walled carbon nanotubes (SWCNT) is proposed. This approach relies on the drain current (I_d) responses of the transistor upon interactions of IL-6 with its corresponding antibody (IL-6R) immobilized on SWCNT. The proposed immunosensor exhibits superior sensitivity (limit-of-detection = 1.37 pg/mL) in virtue of the reduced tube-to-tube contact resistance, good selectivity (no responses to bovine serum albumin and cysteine were observed and detection of target molecules in serum was achieved) as a result of the highly specific interaction between IL-6 and IL-6R, and excellent stability (no significant degradation in the electronic performance after storage under ambient conditions for up to 3 months) in virtue of the strong adhesion of CNT to the quartz substrate and good horizontal alignment of these tubes. Therefore, the proposed immunosensor is a promising platform for early diagnosis of various diseases (including some cancers) that can be indicated by the circulating level of IL-6.

1. Introduction

Interleukin-6 (IL-6, protein structure shown in Fig. S1 in the Supporting Information) is a pleiotropic cytokine that regulates cell growth and differentiation of various tissues. It is known particularly for its role in the immune response and acute phase reactions [1]. As a major mediator of the inflammatory response [2], IL-6 plays a key role in the inflammatory process by acting as both pro-inflammatory cytokine and anti-inflammatory myokine [3]. The anti-inflammatory effect of IL-6 is mediated through its inhibition on tumor necrosis factor (TNF-α) and interleukin 1 (IL-1), and activations of interleukin-1 receptor antagonist (IL-1RA) and interleukin-10 (IL-10) [4]. It has been demonstrated that the dysregulation (in most cases, overexpression) of IL-6 is involved in the pathogenesis of a variety of diseases such as rheumatoid arthritis [5], myeloma [6] and even cancers [7]. More recently, IL-6 has been related to sports science as the circulating level of IL-6 increases in a near-exponential pattern (it precedes the appearance of other cytokines in the circulation) with the intensity and the duration of exercise and training [8], and the working skeletal muscle has been identified as the major source [9]. This can be explained by the fact that IL-6 level is elevated in response to muscle contractions. For this reason, IL-6 can be used as an indicator of the glycogen level in the muscles and a stimulator of glucose metabolism when the glycogen level is low [10]. Furthermore, non-invasive capillary blood sampling, which is more applicable for real-time and point-of-care testing, has been proven to be of the same effectiveness as conventional venous blood sampling for the measurement of plasma IL-6 [11]. This phenomenon is of great significance as it indicates a great potential of IL-6 for real-time monitoring of fatigue that is related to exercises and trainings.

Owing to its diverse biological roles, IL-6 has been targeted by a variety of assays [12–14]. As shown in Table 1, different immunosensing assays targeting at IL-6 detection have been reported, including electrochemical assays [15], florescence-based assays [16] and surface plasmon resonance based assays [17]. Among all assays reported, the enzyme-linked immunosorbent assay (ELISA) [18] and the Western blot method [19] are most widely used ones. ELISA can provide superior sensitivity (limit-of-detection (LOD) < 1 pg/mL), while the Western blot method exhibits excellent selectivity and specificity. However, ELISA is a resource intensive (expensive equipment and well-trained personnel required) method, thus not ideal for practical applications; the Western blot method is a non-quantitative method which provides limited information on the concentration of the analyte targeted [20].

* Corresponding author at: School of Materials Science and Engineering, Nanyang Technological University, 639798, Singapore.
E-mail address: MIYTOK@e.ntu.edu.sg (A.I.Y. Tok).

http://dx.doi.org/10.1016/j.matdes.2015.11.029
0264-1275/

Table 1
A comparison of assays reported for detection of interleukin-6 (IL-6).

Assay	Sensitivity	Advantages	Drawbacks
Enzyme-linked immunosorbent assay (ELISA)	<1 pg/mL	Superior sensitivity	Intensive resources required
Western blot	N.A.	Good selectivity	Non-quantitative assay
Electrochemical immunoassay [15]	1 pg/mL	Label-free, good sensitivity	Sophisticated procedure needed
Fluorescence-based immunoassay [16]	20 pg/mL	Simple assay design	Labeling required
Surface plasmon resonance (SPR) immunoassay [17]	700 pg/mL	Label-free, rapid response	Low sensitivity

Herein, a facile, sensitive, and label-free assay for IL-6 using liquid-gated field-effect transistors (FET) based on horizontally aligned single-walled carbon nanotubes (SWCNT) is proposed. A schematic illustration of the proposed FET sensor is shown in Fig. 1. In the sensing process, binding of the target analyte (e.g. a ligand) in the gate region will cause a change in the conductance of the transducing layer, which is indicated by a change in the drain current (I_d). This change is measured and used as an electrical signal [21–24]. The reported liquid-gated FET biosensors offer real-time monitoring of biomolecules with superior sensitivity and device stability. In virtue of the unique characteristics such as excellent electrical conductance and ultrahigh length-to-diameter ratio, carbon nanotubes have been widely utilized for biosensing applications [25]. In the past decade, real time electronic detections of various biomolecules using functionalized CNT-based FET have been reported [26]. Previously, Palaniappan et al. [27] proposed a transistor based on horizontally aligned CNT for electronic detection of prostate specific antigen (PSA), a potential biomarker of the prostate cancer. Owing to the reduced tube-to-tube contact resistance, the proposed device demonstrated facile and highly sensitive detection of PSA. In this article, we propose a horizontally aligned CNT-based FET sensing platform for real time measurements of IL-6. The proposed platform showed excellent sensitivity (limit-of-detection = 1.37 pg/mL, comparable to ELISA and other assays) and good selectivity. Detection of target molecules in diluted serum (rabbit serum diluted by 100 times with buffer) was also achieved. 1 pg/mL IL-6 in serum triggered a detectable I_d response, indicating that the sensitivity of the serum testing is comparable to that of the buffer testing. Additionally, the devices developed exhibited good stability under ambient conditions for up to 3 months as no major degradation in electronic performance was observed. Considering the cost-effectiveness of the raw materials involved and the facile synthesis routes available for the growth of horizontally aligned CNT on quartz substrates in virtue of the significant advances recently, this IL-6 assay exhibits a great potential for point-of-care applications in the future.

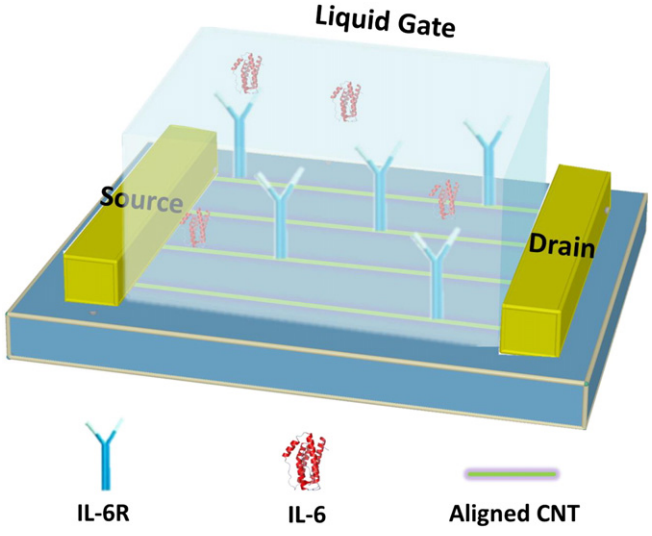

Fig. 1. Schematic illustration of the liquid-gated field-effect transistor sensor based on horizontally aligned single-walled carbon nanotubes for interleukin-6 detections. Interleukin-6 antibodies were immobilized on carbon nanotubes to captured interleukin-6 molecules.

2. Experimental

2.1. Materials

The IL-6 antigen and antibody (specifications shown in the supporting information) were obtained from Sino Biological Inc., Beijing, China. The catalyst, $Co(C_2H_3O_2)_2 \cdot 4H_2O$ (cobalt(II) acetate tetrahydrate, ACS reagent, purity ≥98 wt.%), and other reagents involved in CNT growth were purchased from Sigma-Aldrich Singapore, Singapore and used without further purification. Quartz substrates were obtained from Hoffman Materials LLC. (Carlisle PA, United States) and cut into 1 cm × 1 cm chips. The rabbit serum (R9133) used was purchased from Sigma-Aldrich Singapore, Singapore and used without further purification.

2.2. Growth of CNT by chemical vapor deposition (CVD)

The horizontally aligned CNT were grown on quartz substrates using a modified method based on previous reports [28]. Firstly, quartz substrates were annealed at 900 °C for 8 h. Subsequently, the annealed substrates were sonicated in acetone, isopropyl alcohol and deionized water for 5 min, respectively. Cobalt acetate was deposited on the substrates by a drop-coating method, in which the catalyst was transferred to the substrate using a millimeter-sized brush. To maximize the horizontal alignment of CNT, the catalyst was deposited in a direction perpendicular to the growth direction of CNT. The set-up used for the ethanol CVD process is shown in Fig. S2 (in Supporting Information). Briefly, catalyst-coated substrates were heated to 850 °C under a mixture flow of Ar (200 sccm) and H_2 (100 sccm) and kept for 5 min to allow oxidation of catalysts, which were then reduced to pure Co at 925 °C under a mixture flow of Ar (40 sccm) and H_2 (20 sccm) for 10 min. Afterwards, the as-prepared CNT samples were characterized by Field Emission Scanning Electron Microscope (FESEM, JSM-7600F), Atomic Force Microscope (AFM, Dimension 3100) and Raman spectroscopy (WITec Alpha 300 R).

2.3. Fabrication of liquid gated FET sensors

2 mm wide, 100 nm thick Au source and drain electrodes (spacing = 200 μm) were evaporated onto the substrates. Silicon rubber reservoir was generated along the electrodes to confine the test solutions and silver paint was coated for the convenience of probing. Fig. S3 (shown in Supporting Information) shows a typical device fabricated using the proposed methodology. The I-V characteristics of the transistors fabricated were obtained using a methodology similar to a previous report [29]. With a voltage bias (V_d) of 10 mV applied between the source electrode and the drain electrode, the current (I_d) flowing through the SWCNTs was recorded while sweeping the gate voltage (V_g) from −600 mV to 0 mV. I_d–V_d plots at different gate voltages were also recorded for electrical characterization.

2.4. Detection of IL-6

In order to minimize non-specific binding, surface passivation was achieved by incubation with 1% (*v*/*v*) polyethylene glycol (PEG) in phosphate buffer solution (PBS) for 30 min. Then, IL-6 antibodies (IL-6R) were immobilized on the nanotubes using 1-pyrenebutanoic acid succinimidyl ester (PBSE, chemical structure shown in Fig. S4) as linkers [30]. The immobilization was achieved by incubation with 5 mM PBSE (in phosphorous buffer, pH = 7.4) for 1 h, followed by incubation with 5 μg/mL IL-6R. Subsequently, the device was rinsed with PBS for several times to remove loosely bound antibodies. A voltage bias of 10 mV was applied between the source electrode and the drain electrode, while the gate potential was applied via a reference electrode (3 M KCl) (FLEXREF from World Precision Instruments). The devices were incubated with testing solutions (with different concentrations of IL-6) for 15 min each, followed by removal of the solution and incubation with PBS. I_d was monitored (liquid-gated measurement) during the entire process (in testing solutions and buffer).

3. Results and discussion

Fig. 2(a) shows the Field Emission Scanning Electron Microscope (FESEM) image of the carbon nanotubes grown on quartz substrates. It can be observed that the carbon nanotubes in good horizontal alignment were generated on quartz substrates by the method proposed. It has been revealed that good horizontal alignment can significantly reduce the tube-to-tube contact resistance [25], which is one of the key problems associated with random networks of carbon nanotubes. For this reason, the devices based on horizontally aligned CNT showed improved transconductance, sensitivity and ultimately the overall performance as biosensors [31]. Fig. 2(b) shows the Raman spectrum of carbon nanotubes grown on quartz substrates. The Raman spectrum was obtained using a confocal Raman spectroscopy (WITec Alpha 300 R) employing a Nd:YAG 532 nm laser at 30 μW with a spot size of ~1 μm^2 and a CCD detector with 3 cm^{-1} resolution. The laser was focused using a 20× Nikon air objective (NA = 0.4). The peak at 207 cm^{-1} is associated with the quartz substrate [32], while the peak at 359 cm^{-1} is associated with SWCNT [33]. Fig. 2(c) and (d) shows the Atomic Force Microscope (AFM) image of the nanotubes grown on quartz substrates and its corresponding section analysis, respectively. According to Fig. 2(c), the density of nanotubes on the quartz surface is approximately 3–5 tubes/μm, which is comparable to other protocols reported previously [32]. The section analysis shown in Fig. 2(d) reveals that the diameter of nanotubes generated ranges from 1.7 nm to 2.0 nm, while the average tube diameter is measured to be 1.9 nm. Fig. 3 (a) and (b) show the I_d vs. V_g at a drain voltage (V_d) of 10 mV and I_d vs. V_d at different gate voltages (−400 mV, −300 mV, −200 mV and −100 mV), respectively. As observed from Fig. 3(a), the device shows a typical semiconducting behavior in the range of −600 mV to 0 mV, indicating good functionality as a transistor [34]. Additionally, the linear relation between I_d and V_d illustrates Ohmic contacts between the carbon nanotubes and the Au electrodes.

In kinetic measurements, I_d at a fixed gate potential were tracked (I_d vs. time) and the variation of I_d was recorded as the signal. Briefly, the device was exposed to testing solutions containing different concentrations of IL-6 upon immobilization with IL-6R. Then, the device was rinsed with and incubated in PBS. I_d was recorded during the entire process (including exposure to testing solutions and incubation with PBS). As shown in Fig. 4(a), I_d remained unaffected upon rinsing with buffer solution but dropped drastically upon injection of IL-6. More importantly, the I_d response increased with IL-6 concentration of the

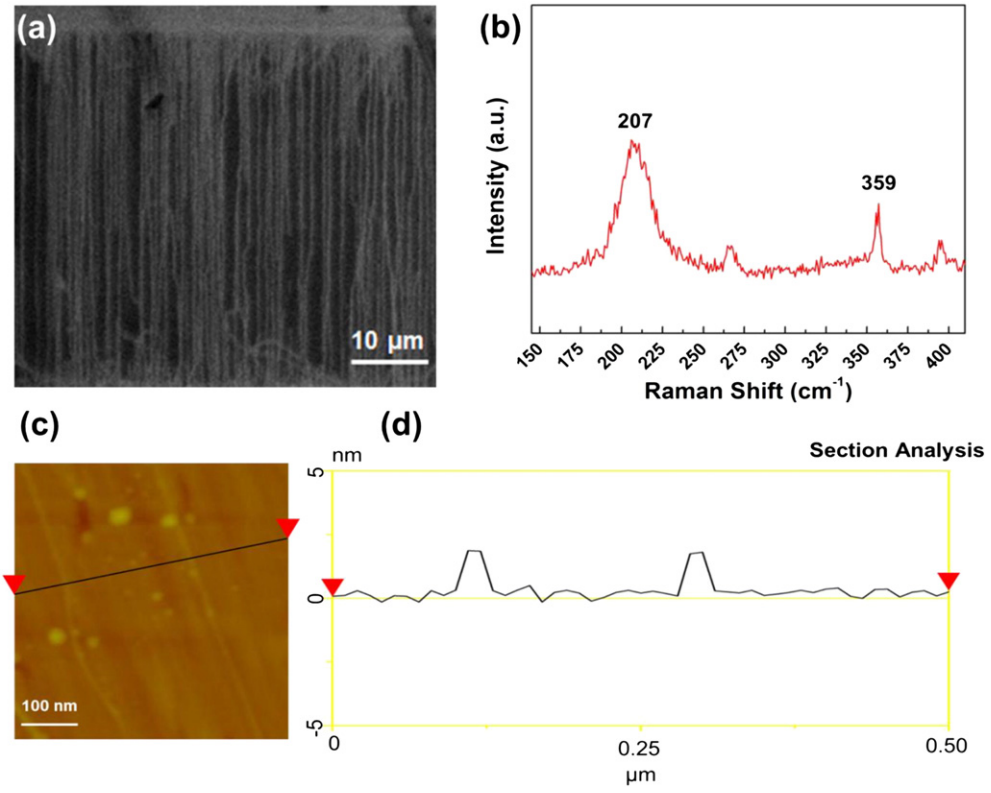

Fig. 2. (a) Field Emission Scanning Electron Microscope (FESEM) image of horizontally aligned CNT on quartz; (b) Raman spectrum of horizontally aligned CNT on quartz substrate (the peak at 207 cm^{-1} corresponds to the quartz substrate and the peak at 359 cm^{-1} is associated with SWCNT); (c) AFM image of horizontally aligned CNT on quartz and (d) its corresponding section analysis.

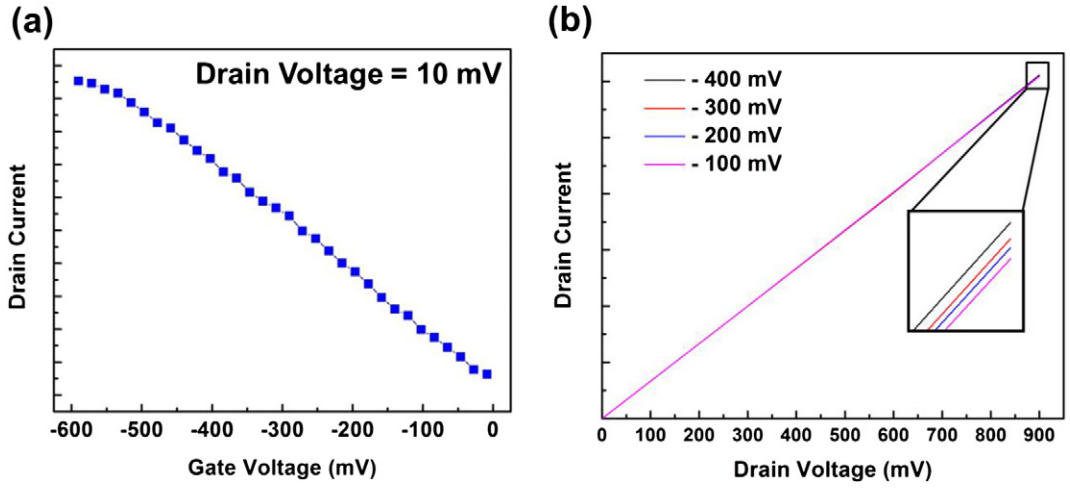

Fig. 3. (a) Drain current vs. gate voltage at a fixed bias voltage (10 mV); (b) drain current vs. drain voltage at different gate voltages (ranging from −400 mV to −100 mV).

testing solution in a logarithmic pattern, as shown in Fig. 4(b). The results suggested that the as-prepared CNT-FET devices are capable of quantitatively measuring IL-6 via the interaction of this molecule with its corresponding antibody (IL-6R in this case). The limit-of-detection calculated by the 3σ/S approach (σ stands for the standard deviation of device response to PBS, which is ~4 nA, and S is the sensitivity, slope of the linear sensor response range; the detailed calculation is shown in the supporting information) [35] is 1.37 pg/mL, which is significantly lower than the circulating level of IL-6 (10–12 pg/mL [36]) and comparable to assays previously reported such as ELISA and electrochemical assays.

The selectivity of as-prepared devices was evaluated by tracking I_d of the immunosensor in response to 100 pg/mL bovine serum albumin (BSA) and 100 pg/mL cysteine. As shown in Fig. 5(a), the I_d responses triggered by 100 pg/mL BSA and 100 pg/mL cysteine were 2.42% and 2.15% respectively, while the responses triggered by 1 pg/mL and 100 pg/mL IL-6 were 4.05% and 18.7% respectively. Neither BSA nor cysteine triggered significant responses compared with IL-6, indicating excellent selectivity of the proposed immunosensor. The superior selectivity can be attributed to the highly specific interaction between IL-6 and its antibody, as well as successful surface passivation prior to kinetic measurements. Furthermore, measurements of IL-6 in serum (rabbit serum diluted with PBS by 100 times) were achieved using the developed devices and the results are shown in Fig. 5(b). As can be seen, I_d responses triggered by IL-6 in serum were detectable and correlated to the concentration of IL-6. The results revealed that detection of IL-6 by the proposed device is highly specific, thus exhibiting a great potential for practical applications.

Additionally, the stability of the developed devices stored under ambient conditions (25 °C and atmosphere pressure) was evaluated. Basically, the electrical performances (I_d vs. V_g curves) of as-prepared devices being stored for different durations were tested and compared with freshly prepared devices. Fig. 6 shows the normalized I_d $\left(\frac{\text{Id at different Vg}}{\text{Id at Vg=0 mV}} \times 100\%\right)$ vs. V_g. ΔI_d in response to the same variation of V_g (−600 mV to 0 mV) were 15%, 14.2%, 13% and 12% for devices after storage for 1 day, 1 week, 1 month and 3 months, respectively. The degradation of sensitivity (in terms of I_d vs. V_g) of the device developed dropped by approximately 20% after storage under ambient conditions for 3 months. Therefore, it can be concluded that the CNT-FET devices developed by the proposed assay exhibit no significant performance degradation after storage under ambient conditions for up to 3 months, indicating excellent stability of these devices. The good stability under ambient conditions makes the proposed device a promising sensing platform for practical applications.

4. Conclusions

A facile, sensitive, and label-free assay for detections of IL-6 using liquid-gated FET sensors based on horizontally aligned SWCNT is

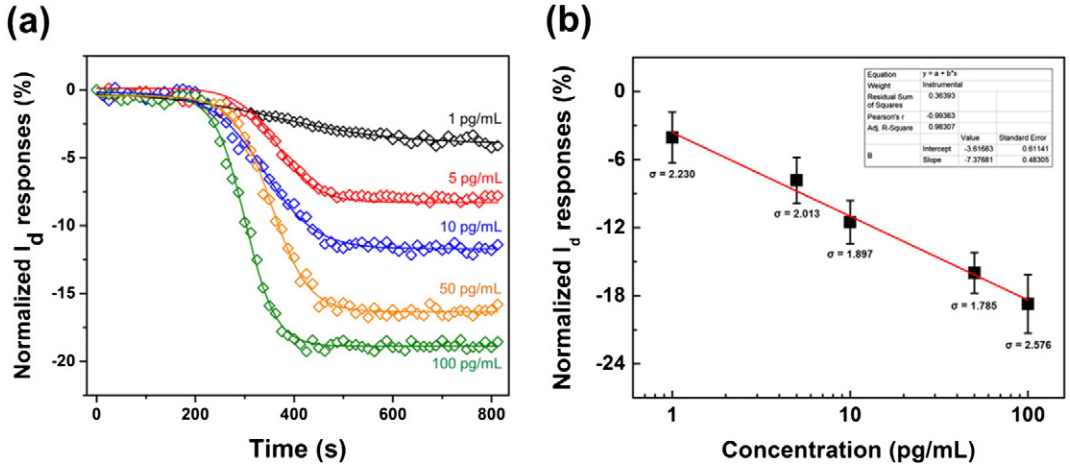

Fig. 4. (a) Kinetic measurement of IL-6 (concentrations ranging from 1 pg/mL to 100 pg/mL) by the proposed immunosensor; (b) average drain current responses of devices from different batches (n > 3).

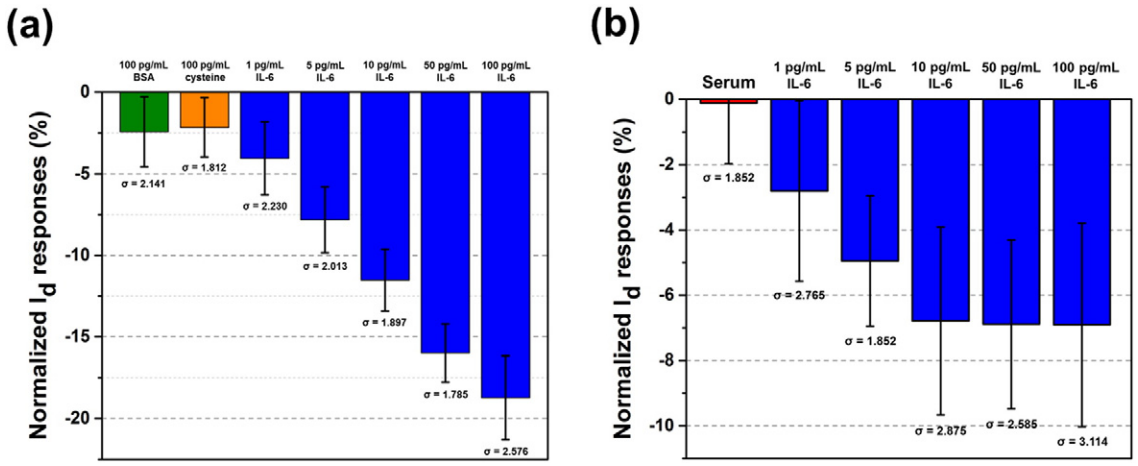

Fig. 5. (a) Drain current responses to 100 pg/mL BSA and 100 pg/mL cysteine as compared to responses triggered by IL-6 (n > 3); (b) measurements of IL-6 in diluted serum using the proposed assay (n > 3).

demonstrated. The proposed device exhibited superior sensitivity (LOD = 1.37 pg/mL) in virtue of the reduced tube-to-tube contact resistance, good selectivity (no responses to BSA and cysteine were observed and detection of target molecules in serum was achieved) as a result of the highly specific interaction between IL-6R and IL-6, and excellent stability (storage under ambient conditions for up to 3 months) due to the strong adhesion of CNT to the quartz substrate and good horizontal alignment of these tubes. The proposed immunosensor shows a great potential for early diagnosis of various diseases indicated by varying circulating level of IL-6.

Acknowledgments

This research was funded by the Institute for Sports Research, Nanyang Technological University.

Appendix A. Supplementary data

Supplementary data to this article can be found online at http://dx.doi.org/10.1016/j.matdes.2015.11.029.

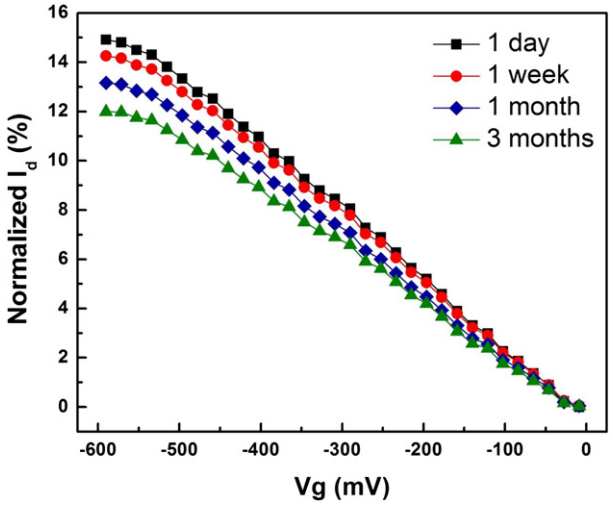

Fig. 6. I_d vs. V_g of devices after storage under ambient conditions for different durations.

References

[1] P. Heinrich, I. Behrmann, G. Muller-Newen, F. Schaper, L. Graeve, Interleukin-6-type cytokine signalling through the gp130/Jak/STAT pathway1, Biochem. J. 334 (1998) 297–314.
[2] J. Gauldie, C. Richards, D. Harnish, P. Lansdorp, H. Baumann, Interferon beta 2/B-cell stimulatory factor type 2 shares identity with monocyte-derived hepatocyte-stimulating factor and regulates the major acute phase protein response in liver cells, Proc. Natl. Acad. Sci. 84 (1987) 7251–7255.
[3] K. Ostrowski, T. Rohde, S. Asp, P. Schjerling, B.K. Pedersen, Pro- and anti-inflammatory cytokine balance in strenuous exercise in humans, J. Physiol. 515 (1999) 287–291.
[4] H. Takizawa, M. Desaki, T. Ohtoshi, T. Kikutani, H. Okazaki, M. Sato, et al., Erythromycin suppresses interleukin-6 expression by human bronchial epithelial cells: a potential mechanism of its anti-inflammatory action, Biochem. Biophys. Res. Commun. 210 (1995) 781–786.
[5] T. Hirano, T. Kishimoto, Interleukin-6: possible implications in human diseases, Res. Clin. Lab. 19 (1989) 1–10.
[6] B. Klein, X.-G. Zhang, M. Jourdan, F. Houssiau, L. Aarden, M. Piechaczyk, et al., Paracrine rather than autocrine regulation of myeloma-cell growth and differentiation by interleukin-6, Blood 73 (1989) 517–526.
[7] D.A. Twillie, M.A. Eisenberger, M.A. Carducci, W.-S. Hseih, W.Y. Kim, J.W. Simons, Interleukin-6: a candidate mediator of human prostate cancer morbidity, Urology 45 (1995) 542–549.
[8] S. Gray, M. Clifford, R. Lancaster, M. Leggate, M. Davies, M. Nimmo, The response of circulating levels of the interleukin-6/interleukin-6 receptor complex to exercise in young men, Cytokine 47 (2009) 98–102.
[9] K. Ostrowski, T. Rohde, M. Zacho, S. Asp, B. Pedersen, Evidence that interleukin-6 is produced in human skeletal muscle during prolonged running, J. Physiol. 508 (1998) 949–953.
[10] D.C. Nieman, J.M. Davis, D.A. Henson, J. Walberg-Rankin, M. Shute, C.L. Dumke, et al., Carbohydrate ingestion influences skeletal muscle cytokine mRNA and plasma cytokine levels after a 3-h run, J. Appl. Physiol. 94 (2003) 1917–1925.
[11] S.H. Faulkner, K.L. Spilsbury, J. Harvey, A. Jackson, J. Huang, M. Platt, et al., The detection and measurement of interleukin-6 in venous and capillary blood samples, and in sweat collected at rest and during exercise, Eur. J. Appl. Physiol. 114 (2014) 1207–1216.
[12] J. Huang, H. Chen, W. Niu, D.W. Fam, A. Palaniappan, M. Larisika, et al., Highly manufacturable graphene oxide biosensor for sensitive Interleukin-6 detection, RSC Adv. 5 (2015) 39245–39251.
[13] J. Huang, J. Harvey, W.D. Fam, M.A. Nimmo, I.A. Tok, Novel biosensor for interLeukin-6 detection, Procedia Eng. 60 (2013) 195–200.
[14] G.-C. Fan, X.-L. Ren, C. Zhu, J.-R. Zhang, J.-J. Zhu, A new signal amplification strategy of photoelectrochemical immunoassay for highly sensitive interleukin-6 detection based on TiO_2/CdS/CdSe dual co-sensitized structure, Biosens. Bioelectron. 59 (2014) 45–53.
[15] T. Li, M. Yang, Electrochemical sensor utilizing ferrocene loaded porous polyelectrolyte nanoparticles as label for the detection of protein biomarker IL-6, Sensors Actuators B Chem. 158 (2011) 361–365.
[16] X. Hun, Z. Zhang, Functionalized fluorescent core–shell nanoparticles used as a fluorescent labels in fluoroimmunoassay for IL-6, Biosens. Bioelectron. 22 (2007) 2743–2748.
[17] T.-H. Chou, C.-Y. Chuang, C.-M. Wu, Quantification of Interleukin-6 in cell culture medium using surface plasmon resonance biosensors, Cytokine 51 (2010) 107–111.
[18] M. Helle, L. Boeije, E. de Groot, A. de Vos, L. Aarden, Sensitive ELISA for interleukin-6: detection of IL-6 in biological fluids: synovial fluids and sera, J. Immunol. Methods 138 (1991) 47–56.
[19] J.J. Senn, P.J. Klover, I.A. Nowak, R.A. Mooney, Interleukin-6 induces cellular insulin resistance in hepatocytes, Diabetes 51 (2002) 3391–3399.

[20] D.J. MacPhee, Methodological considerations for improving Western blot analysis, J. Pharmacol. Toxicol. Methods 61 (2010) 171–177.
[21] A. Palaniappan, W. Goh, D. Fam, G. Rajaseger, C. Chan, B. Hanson, et al., Label-free electronic detection of bio-toxins using aligned carbon nanotubes, Biosens. Bioelectron. 43 (2013) 143–147.
[22] J. Huang, D. Fam, Q. He, H. Chen, D. Zhan, S.H. Faulkner, et al., The mechanism of graphene oxide as a growth template for complete reduced graphene oxide coverage on an SiO_2 substrate, J. Mater. Chem. C 2 (2014) 109–114.
[23] J. Huang, M. Larisika, D. Fam, Q. He, M.A. Nimmo, C. Nowak, et al., The extended growth of graphene oxide flakes using ethanol CVD, Nanoscale (2013).
[24] M. Paradise, T. Goswami, Carbon nanotubes — production and industrial applications, Mater. Des. 28 (2007) 1477–1489.
[25] M.E. Roberts, M.C. LeMieux, Z. Bao, Sorted and aligned single-walled carbon nanotube networks for transistor-based aqueous chemical sensors, ACS Nano 3 (2009) 3287–3293.
[26] R.J. Chen, S. Bangsaruntip, K.A. Drouvalakis, N.W.S. Kam, M. Shim, Y. Li, et al., Noncovalent functionalization of carbon nanotubes for highly specific electronic biosensors, Proc. Natl. Acad. Sci. 100 (2003) 4984–4989.
[27] A. Palaniappan, W. Goh, J. Tey, I. Wijaya, S. Moochhala, B. Liedberg, et al., Aligned carbon nanotubes on quartz substrate for liquid gated biosensing, Biosens. Bioelectron. 25 (2010) 1989–1993.
[28] L. Huang, X. Cui, B. White, S.P. O'Brien, Long and oriented single-walled carbon nanotubes grown by ethanol chemical vapor deposition, J. Phys. Chem. B 108 (2004) 16451–16456.
[29] M. Kruger, M. Buitelaar, T. Nussbaumer, C. Schonenberger, L. Forro, Electrochemical carbon nanotube field-effect transistor, Appl. Phys. Lett. 78 (2001) 1291–1293.
[30] R.J. Chen, Y. Zhang, D. Wang, H. Dai, Noncovalent sidewall functionalization of single-walled carbon nanotubes for protein immobilization, J. Am. Chem. Soc. 123 (2001) 3838–3839.
[31] T. Reid, Nanotube arrays: bridging the gap, Nat. Nanotechnol. (2007).
[32] C. Kocabas, S.J. Kang, T. Ozel, M. Shim, J.A. Rogers, Improved synthesis of aligned arrays of single-walled carbon nanotubes and their implementation in thin film type transistors, J. Phys. Chem. C 111 (2007) 17879–17886.
[33] A. Rao, E. Richter, S. Bandow, B. Chase, P. Eklund, K. Williams, et al., Diameter-selective Raman scattering from vibrational modes in carbon nanotubes, Science 275 (1997) 187–191.
[34] A. Kojima, C.K. Hyon, T. Kamimura, M. Maeda, K. Matsumoto, Protein sensor using carbon nanotube field effect transistor, Jpn. J. Appl. Phys. 44 (2005) 1596.
[35] L. Torsi, G.M. Farinola, F. Marinelli, M.C. Tanese, O.H. Omar, L. Valli, et al., A sensitivity-enhanced field-effect chiral sensor, Nat. Mater. 7 (2008) 412–417.
[36] A. Marques-Deak, G. Cizza, F. Eskandari, S. Torvik, I.C. Christie, E.M. Sternberg, et al., Measurement of cytokines in sweat patches and plasma in healthy women: validation in a controlled study, J. Immunol. Methods 315 (2006) 99–109.